SPRING ELEMENT MODEL FOR HYBRID COMPOSITES WITH A RANDOM FIRE PACKING

Rodrigo P. Tavares[1], Fermin Otero[2], Albert Turon[3] and Pedro P. Camanho[4]

[1] DEMec, Faculdade de Engenharia da Universidade do Porto, Porto,Portugal; AMADE, Polytechnic School, University of Girona, Girona, Spain; INEGI, Instituto de Ciência e Inovação em Engenharia Mecânica e Engenharia Industrial, Porto, Portugal; rptavares@inegi.up.pt
[2] INEGI, Instituto de Ciência e Inovação em Engenharia Mecânica e Engenharia Industrial, Porto, Portugal; fotero@inegi.up.pt
[3] AMADE, Polytechnic School, University of Girona, Girona, Spain; Albert.Turon@udg.edu
[4] DEMec, Faculdade de Engenharia da Universidade do Porto, Porto,Portugal; INEGI, Instituto de Ciência e Inovação em Engenharia Mecânica e Engenharia Industrial, Porto, Portugal; pcamanho@fe.up.pt

Keywords: Composites, Fracture, Strength, Numerical modelling

ABSTRACT

An efficient computational model to simulate tensile failure of both non-hybrid and hybrid composites is proposed. This model is based on the spring element model, which is extended to a random 2D fibre packing and hybrid composites, with different fibre properties. The proposed model is used to study the local stress fields around a broken fibre as well as the failure process in composite materials. The influence of fibre strength distributions and matrix properties on this process is also analysed. The numerical results obtained are in good agreement with the experimental data.

1 INTRODUCTION

Modelling the longitudinal tensile failure of unidirectional (UD) composite materials is a challenging task due to the complex mechanisms that govern this type of failure. As the main load carrying component, the fibres play an important role in the failure process. It is understood that fibre strength is a stochastic property that is dominated by a distribution of flaws [1,2], therefore, an accurate characterization of the random nature of fibre strength is necessary to develop proper composite models.

Another important factor in the failure process is the stress redistribution once a fibre is broken and the interaction between multiple fractures leading to the formation of clusters of broken fibres [3–6]. When a fibre breaks it does not fully lose its load carrying capability because the surrounding matrix is loaded in shear and transfers stress back onto the unbroken fibre part [7,8]. A region along the fibre called ineffective length is created. In this region the fibre's load carrying capability is hampered, however, at a certain distance away from the breakage the fibre stress carrying capability is fully recovered. The well known Cox's shear-lag model can be used to estimate the ineffective length and stress distribution around the broken fibre [9]. However, shear yielding of the matrix at the tip of broken fibre will be initiated due to an intensive stress concentration state. To consider this phenomenon, Kelly and Tyson [10] proposed modelling the matrix behaviour within the ineffective length with a perfect-plasticity model. Therefore, the ineffective length is calculated from the load balance between the fibre and matrix. The axial fibre stress recovery is a linear function of the distance to the fracture plane. Following this ideas, the Global Load Sharing (GLS) model was proposed by Curtin [11]. In this approach, the stress released from a broken fibre is equally distributed among the remaining unbroken fibres. GLS models do not take into account the interaction between the fibres and no local fields due to fibre fracture are considered. Local Load Sharing (LLS) models were developed to take into account fibre interaction in the longitudinal failure of UD composites [12]. Several analytical models to determine the stress concentration factor around a single broken fibre [8] or in the presence of multiple broken fibres [13]have been proposed. On the other hand, 3D Finite Element Models (3D FEM) have been used to fully model the microstructure of the composite [14,15]. However, these models are

computationally expensive due to the refined meshes involved and the complex material models required, imposing a limitation in the number of fibres represented in the Representative Volume Element (RVE).

The Spring Element Model (SEM) was proposed by Okabe and co-workers as a low computational cost alternative to 3D FEM [16,17]. The SEM takes into account local stress redistribution due to fibre failure. The model is based on the assembly of periodic packages of fibre and matrix spring elements. The periodic package or unit cell consists of one fibre surrounded by six other fibres connected through shear spring elements that represent the matrix behaviour. Therefore, the unit cell consists of fibre axial springs in the longitudinal direction and matrix shear springs in transverse direction. This modelling approach has the advantage of being computationally efficient, allowing the simulation of RVEs with a large number of fibres, while allowing to accurately capture the stress redistribution and fibre break interaction during the failure process of UD composites.

The correct representation of the mechanics of longitudinal tensile failure is also important for the development of new material systems, such as fibre-hybrid composites. Fibre hybridisation is a strategy that can lead to improved composite properties and performance. Not only the material properties are changed but also the damage propagation mechanisms leading to final failure [18]. However, the different properties of the hybridized fibres and the more complex geometry of these materials make it more difficult to predict their tensile behaviour as well as understand the fibre fracture process. Zweben [12] was the first to extend the shear-lag model for hybrid composites, which was later improved by [19]. However, these models only consider a 1D array of fibres and are unable to be used to study the effect of hybrid volume fraction. Recently, Mishnaevsky and Dai [20] developed a model with a 2D fibre packing to study the influence of fibre dispersion in the damage development. Swolfs et al. [21] developed a Monte Carlo based model to address the effect of fibre dispersion on the hybrid effect, however, Swolfs' simplified model considers a regular fibre packing and a very local load sharing stress redistribution scheme. In a recent work[15] , Tavares et al. developed a fully 3D micromechanical model capable of capturing the main failure mechanisms in both non-hybrid and hybrid composites. These models are computationally expensive and the size of the RVE is limited to only a few fibres.

The objective of this work is to present a simple, yet accurate and computationally efficient model to predict the failure behaviour for both non-hybrid and hybrid composites using a random fibre distribution. The model should be able to capture the clustering process leading to the ultimate failure of UD composites. The influence of different material properties and the stress redistribution on the failure process for non-hybrid composites is analysed in detail.

2 SPRING ELEMENT MODEL FOR RANDOM DISTRIBUTION OF DIFFERENT FIBRES

The model proposed in this section is an extension of the SEM approach to both, random distribution of fibres and hybrid composites, where fibres can have different geometrical and mechanical properties. The SEM consists of longitudinal spring elements, which represent the fibres, connected by transverse spring elements representing the matrix. The matrix contribution in the axial load, i.e. fibre direction, is disregarded in SEM, which is a commonly accepted hypothesis for UD polymer composites. Therefore, only the matrix shear contribution is represented through shear transverse elements.

To obtain the geometric model necessary to represent the composite's micro-structure, a periodic 3D RVE is generated with a random fibre distribution, using the random generator developed by Melro et al. [22] with the necessary modifications. To guarantee that the RVE has a defined quadrangular geometry, the fibres that are divided by the boundary of the RVE are forced to have its centre at the edge, while ensuring geometric periodicity. With the centre of the fibres defined, ensuring the correct fibre volume fraction and that no fibre overlap occurs, a 2D Delaunay triangulation algorithm is used to

generate a 2D triangular mesh. Figure 1 shows an example of a mesh, where each circle represents a fibre and each line a matrix shear element. Finally, to generate the 3D RVE mesh the previously obtained 2D mesh is replicated with an offset distance of l^z, which is the predetermined length for fibre spring elements, until the final total desired length of the RVE in fibre direction is achieved. The generated sections are connected through longitudinal fibre spring elements.

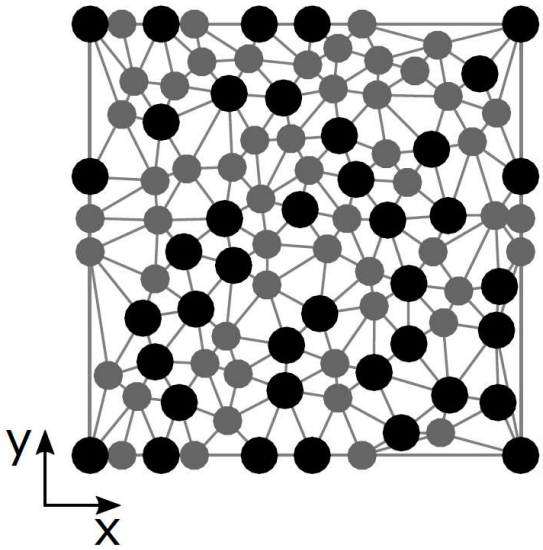

Figure 1: 2D mesh for a periodic RVE with a random fibre distribution.

The stiffness matrix for the fibre elements is unchanged from Okabe's SEM and is given by:

$$\boldsymbol{K_f^e} = \frac{A_f^e E^e}{l^z}\begin{bmatrix} 1 & -1 \\ -1 & 1 \end{bmatrix} \tag{1}$$

where A_f is the fibre area, E_f the fibre's Youngs modulus and l_z the longitudinal element lengthg. The superscript e refers to element properties or parameters, which can be different for the different fibres involved.

Due to the random distribution of the fibres, two major changes occur with respect to the hexagonal packing used in the original SEM: firstly the distance between each fibre element differs and secondly not all fibre elements are connected to other six fibres, as in the hexagonal packing. They can be connected to from five to eight fibres. Therefore, the stiffness of the matrix elements change from element to element. This makes it necessary to change the approach to obtain the stiffness matrix of the matrix shear elements, which results in:

$$\boldsymbol{K_m} = \frac{G\left(A_m^{(2)} - A_m^{(1)}\right)}{d\ln\left(A_m^{(2)}/A_m^{(1)}\right)}\begin{bmatrix} 1 & -1 \\ -1 & 1 \end{bmatrix} \tag{2}$$

where G is the matrix shear modulus, $A_m^{(1)}$ and $A_m^{(2)}$ are the effective areas from fibre 1 and 2 that are connected by the matrix element and d is the distance between the surfaces of both connected fibres.

To be able to predict the failure of the composite material it is necessary to define failure criteria for

the fibre elements as well as the matrix elements.

For the fibre elements a failure criteria associated with the longitudinal failure mechanism is considered, which can be written in its general form as:

$$\frac{\sigma_f}{X_T^c} - 1 < 0 \text{ if } \sigma_f > 0 \tag{3}$$

where σ_f is the fibre stress and X_T^c is the tensile strength in the fibre element. This strength is assigned randomly to each element of the RVE according to an appropriate statistical distribution. In the present implementation of the proposed model a fibre element will be considered fully damaged if the failure criteria given by Eq. 3 is not satisfied. Therefore, when a fibre element does not verify Eq. 3 it is considered broken and the number of broken fibres is updated accordingly.

Fibre-matrix interface debonding has been shown to have a large influence on the tensile failure of UD composites [15,23]. To take this into account, a failure criterion was implemented for the matrix shear elements. The implemented failure criterion is a simple maximum shear stress criterion:

$$\frac{|\sigma_m|}{\tau^u} - 1 < 0 \tag{4}$$

where σ_m is the matrix shear stress and τ^u is the fibre-matrix interfacial strength. Similarly to what was done for the fibre, no damage evolution was considered in this failure process. Therefore, it was considered that when the failure criterion is achieved the matrix element is broken and looses all its load carrying capability. This causes a disconnection between both fibres previously connected by the matrix element and, therefore, there is no load transfer between them.

It is interesting to note that in this model, and on the contrary to what was done by [16] in the original SEM, the stresses on the fibre elements in the ineffective length are not imposed, but are obtained from the overall equilibrium of the system together with the failure criterion proposed for the matrix shear elements.

3 NUMERICAL RESULTS

3.1 Local fields around a broken fibre

To verify if the model is capable of correctly capturing the stress profile of a broken fibre, several simulations were performed using an RVE with a transverse section of 87.5x87.5 μm composed of 132 fibres with a length of 350 μm. The fibres used for these simulations are the AS4 carbon fibres[24], whose properties are: E_f=234 GPa, R_f=3.5 μm.

The ineffective length of a broken fibre in this model is not only controlled by the shear modulus of the matrix (G) but also by the fibre-matrix interfacial strength (τ^u), which is associated with debonding. Figure a shows the influence of the matrix shear modulus and the consideration of debonding in the stress recovery profile of a broken fibre. For comparison purposes the Kelly-Tyson [10] and modified Cox [9] shear-lag models are shown, using a fibre-matrix interfacial strength of 70 MPa and a matrix shear modulus of 1 GPa. The results shown were obtained considering an applied strain of 2\%. When a fibre breaks, there is not only an ineffective length in the broken fibre, but the stress previously carried by this fibre is redistributed among the surrounding intact fibres, increasing the stress carried by these fibres and thus increasing their failure probability. The increase of stress can be quantified by a Stress Concentration Factor (SCF), considered here to be the ratio of the actual stress in the fibre over the stress in the fibre if there were no breaks. This SCF is affected by the matrix and fibre properties as well as by the fibre arrangement. Figure 2 shows the SCF as a function of the distance between the centre of a given fibre and the centre of the broken fibre, in the fracture plane. The results are shown for matrix

shear moduli of 1 and 2 GPa and without a limit on the maximum shear stress and with a fibre-matrix interfacial strength of τ^u 70 MPa.

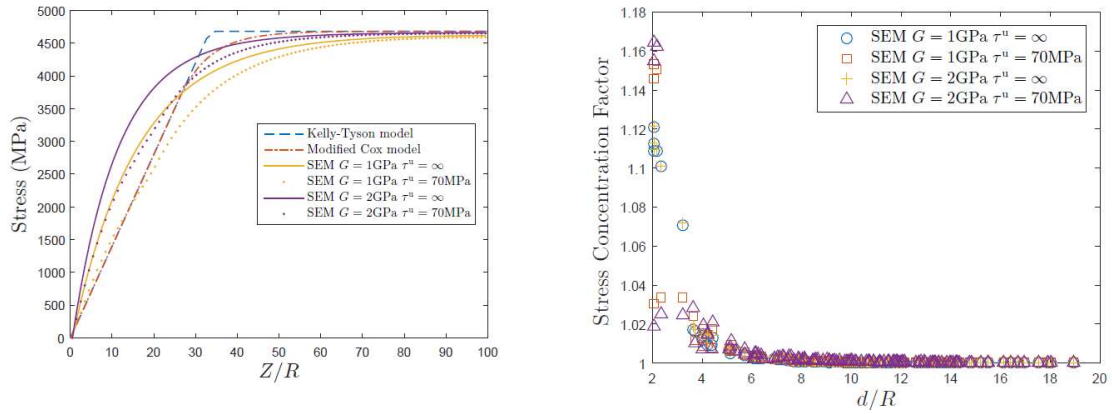

Figure 2: Influence of matrix properties on the stress recovery profile of a broken fibre (left); Stress concentrations as a function of the distance to the broken fibre (right).

It can be observed in Figure that the stress recovery profile of a broken fibre is captured by the model. While there are some differences between the stress profile obtained by the SEM and the simplified shear-lag models, the profile is considered to be accurate and therefore there is no need to superimpose the shear-lag profile in the modelling strategy. It is also possible to see that the SCF decreases away from the broken fibre, being this decrease continuous if no debonding is considered. If debonding is considered the stress redistribution is more complex as there is a maximum matrix shear stress in the matrix shear elements, causing the stress redistribution to be less uniform and more dependent on the actual fibre arrangement.

3.2 Influence of the fibre strength distribution

The tensile failure of composite materials is a fibre dominated process, therefore, it is necessary to accurately capture the fibre's stochastic strengths. Fibres exhibit weakest-link characteristics and their strength is flaw dominated. The most used statistical distribution to describe the strength of the fibres is the Weibull distribution:

$$P(\sigma) = 1 - e^{\left(\left(\frac{L}{L_0}\right)\left(\frac{\sigma}{\sigma_0}\right)^{\rho}\right)} \tag{5}$$

where P is the failure probability at the applied stress σ, L is the characteristic gauge length, σ_0 and ρ are the Webull scale and shape parameters at the reference length L_0. Although being the most used statistical distribution for fibre strength, it has been shown that the Weibull distribution is not the best suited for carbon and glass fibres. To better capture the experimental data different distributions have been proposed, usually based on the Weibull distribution such as the Power-Law Accelerated Weibull (PLAW) [24–26]:

$$P(\sigma) = 1 - e^{\left(\left(\frac{L}{L_0}\right)^{\alpha}\left(\frac{\sigma}{\sigma_0}\right)^{\rho}\right)} \tag{6}$$

where α is an additional parameter for the distribution. Curtin [24] proposed another model entitled Weibull of Weibulls (WOW) that conforms with Equation (6) but with more solid physical background. This model assumes that the strength distribution along a fibre is a Weibull distribution with modulus ρ' and that the characteristic strength of each fibre follows a different Weibull distribution with modulus m. The different characteristic strengths of the fibres are attributed to the processing and handling of the fibres. The difference between the PLAW and WOW models is that, in the WOW model the strength along an individual fibre is highly correlated, leading to very weak and very strong fibres, while in the

PLAW model there is no direct correlation in the strength of the elements within a single fibre.

Several simulations using different random distributions were performed using each of the presented strength distributions. The models used have approximately 1100 fibres, with a length of $1.05mm. For the WOW strength distribution, five simulations with a periodic hexagonal fibre arrangement were also simulated. A summary of some relevant results of the simulations are shown in Table 1.

Table 1: Maximum stress, failure strain and maximum cluster size for the AS4 composite using different strength distributions and fibre distribution.

	Sim.	1	2	3	4	5	Avg.	STDV
Weibull	X_T (MPa)	3365	3436	3370	3369	3366	3381	30.78
	ε_f (%)	2.74	2.82	2.64	2.75	2.64	2.72	0.08
	Max. cluster	23	29	14	28	19	23	6.27
PLAW	X_T (MPa)	2117	2095	2125	2137	2105	2116	16.41
	ε_f (%)	1.71	1.76	1.72	1.73	1.71	1.73	0.02
	Max. cluster	15	33	24	25	23	24	6.40
WOW	X_T (MPa)	1939	1978	1948	1928	1961	1951	19.61
	ε_f (%)	1.65	1.73	1.66	1.68	1.65	1.67	0.03
	Max. cluster	20	27	36	19	16	23	8.02
WOW hexag.	X_T (MPa)	1934	1958	1938	1930	1947	1941	11.21
	ε_f (%)	1.67	1.66	1.61	1.61	1.68	1.65	0.03
	Max. cluster	40	34	20	22	45	32	10.96

The stress-strain curves for all the simulations are shown in Figure 3. The traditional Weibull distribution leads to a higher composite strength prediction, when compared with PLAW and WOW distributions. This is due to the large difference between $\underline{L_0}$ and $L=F$, which leads to a higher individual tensile strength of the fibre elements. Using the PLAW or WOW model leads to lower tensile strengths, as the length scaling is affected also by the α parameter, leading to a reduction of the elements individual tensile strength and, therefore, to a reduction of predicted composite tensile strength.

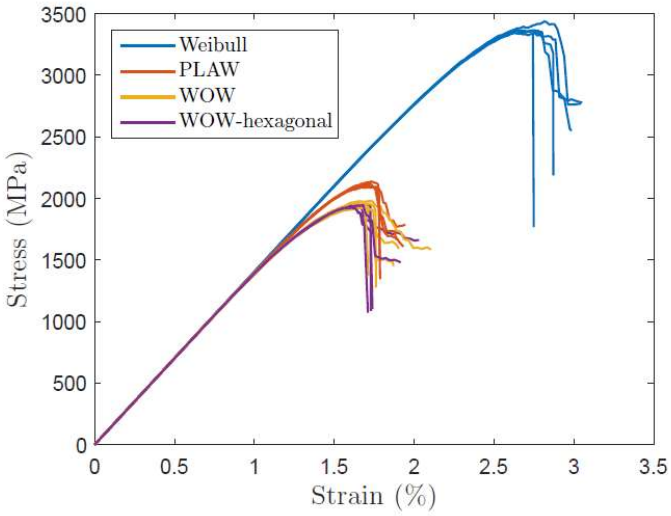

Figure 3 Stress-strain curves for AS4 composites using different strength distributions.

3.3 Cluster formation

The model proposed here can also be used to analyse the development of clusters of broken fibres during the failure process. A cluster is defined following [6]: two fibres are considered to be part of the

same cluster if (i) the distance between the centres of the two fibres is lower than four times the fibre radius and (ii) the axial distance between break planes was less than ten times the fibre radius. The maximum cluster size for each simulation using the three different strength distributions is shown in Table 1. The maximum cluster size does not significantly change with the different strength distributions, being this maximum around 23-24 fibres in average. However, there are simulations where it has gone as high as 36 fibres and as low as 14 fibres, due to the randomness of the element strength assignment. Although the cluster size does not change with the strength distribution it changes when comparing the hexagonal and random fibre packings, being the mean maximum cluster size in the hexagonal packing equal to 32 while for the random packing is 23. The mean maximum cluster size considering a random fibre packing is higher than the one observed experimentally by [5], who determined a maximum cluster size of 14 broken fibres for a T700 carbon fibre based composite.

To better understand the fibre fracture process and the cluster formation, the fibre break density in each section of the RVE is plotted in Figure 4 In this figure it is possible to see the stress-strain curve as well as the percentage of broken fibres in each section of the RVE for all the sections along the fibre direction for three different applied strains, which are marked in the stress-strain curve. The microstructures shown represent the broken fibres within 10 fibre radius in each direction of the critical section. This critical section was considered the one that had a higher fibre break density before the final failure of the composite, which was at Z=0.868 mmThe critical section and the 10 fibre radius distance in each direction are plotted in the fibre break density image in full and dashed lines. In the microstructure in blue it is possible to see that there are a several broken fibres forming clusters, which grow with applied strain until the critical strain is achieved (figure in orange) leading to the failure of the material. After its failure (in green) it is possible to see that a large percentage of the fibres are broken and, therefore, the composite looses the load carrying capability.

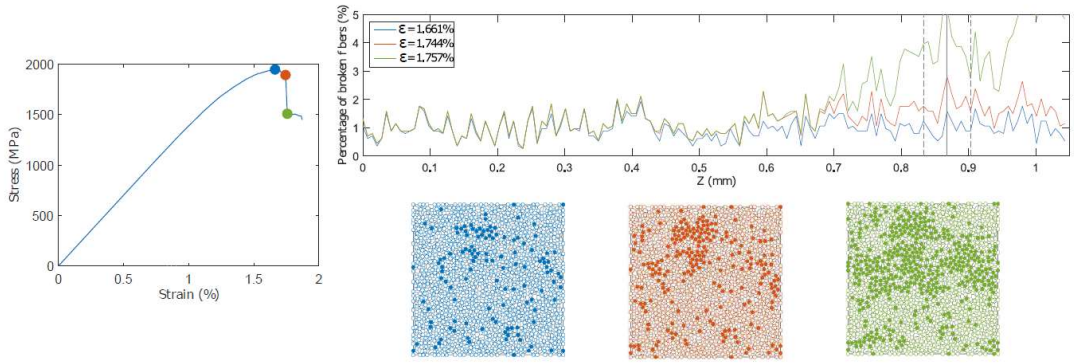

Figure 4: Stress-strain curve of the AS4 composite with a WOW distribution, accompanied by the fibre break density in each section of the composite and the microstructures at the critical section at different stages.

4 CONCLUSIONS

A spring element model that takes into account a random fibre packing and that can be used for fibre hybrid composites has been presented. The model is able to accurately capture the local stress fields surrounding a broken fibre, capturing the ineffective length of a broken fibre as well as the stress concentrations in the intact fibres that surround a broken one. Unlike other models present in the literature, the stress redistribution coming from a fibre break is not enforced and the resulting stress concentrations in the surrounding fibres arise due to the solution of the global system of equations that governs the problem. Fibre matrix debonding is inherently captured due to the incorporation of a maximum shear stress criterion into the matrix spring elements.

As a fibre dominated failure, the tensile failure of unidirectional composites largely depends on the

accurate representation of the strength of the fibre elements. Several statistical distributions for fibre strength are available in the literature. To study their influence on the tensile behaviour of composites several simulations were performed using the traditional Weibull, the Power Law Accelerated Weibull and the Weibull of Weibulls strength distributions. The results were compared with the available experimental data and it was concluded that the Weibull of Weibulls fiber strength distribution leads to more accurate results.

The developed model was used in this work for non-hybrid composites, with a single fibre type, however, the developed framework can be used for hybrid composites, with more than one fibre type. This possibility will be analysed by the authors in a future work.

4 REFERENCES

[1] Argon AS. Statistical Aspects of Fracture. In: Broutman LJ, editor. Compos. Mater. Fatigue Fract., vol. 5, New York: Academic Press; 1974, p. 153–90.

[2] Lamon J. Mécanique de la rupture fragile et de l'endommagement: approches statistiques et probabilistes. Hermes Science Publications; 2007.

[3] Thionnet A, Chou HY, Bunsell A. Fibre break processes in unidirectional composites. Compos Part A Appl Sci Manuf 2014;65:148–60. doi:http://dx.doi.org/10.1016/j.compositesa.2014.06.009.

[4] Pimenta S. Fibre failure modelling. In: Camanho PP, Hallet SR, editors. Numer. Model. Fail. Adv. Compos. Mater., Woodhead Publishing; 2015.

[5] Scott AE, Mavrogordato M, Wright P, Sinclair I, Spearing SM. In situ fibre fracture measurement in carbon–epoxy laminates using high resolution computed tomography. Compos Sci Technol 2011;71:1471–7. doi:10.1016/j.compscitech.2011.06.004.

[6] Swolfs Y, Morton H, Scott AE, Gorbatikh L, Reed PAS, Sinclair I, et al. Synchrotron radiation computed tomography for experimental validation of a tensile strength model for unidirectional fibre-reinforced composites. Compos Part A Appl Sci Manuf 2015;77:106–13. doi:10.1016/j.compositesa.2015.06.018.

[7] Fukuda H. Stress concentration factors in unidirectional composites with random fiber spacing. Compos Sci Technol 1985;22:153–63. doi:10.1016/0266-3538(85)90082-X.

[8] Hedgepeth JM, Van Dyke P. Local Stress Concentrations in Imperfect Filamentary Composite Materials. J Compos Mater 1967;1:294–309. doi:10.1177/002199836700100305.

[9] Landis CM, McMeeking RM. A shear-lag model for a broken fiber embedded in a composite with a ductile matrix. Compos Sci Technol 1999;59:447–57. doi:10.1016/S0266-3538(98)00091-8.

[10] Kelly A, Tyson WR. Tensile properties of fibre-reinforced metals: Copper/tungsten and copper/molybdenum. J Mech Phys Solids 1965;13:329–50. doi:10.1016/0022-5096(65)90035-9.

[11] Curtin WA. Exact theory of fibre fragmentation in a single-filament composite. J Mater Sci 1991;26:5239–53. doi:10.1007/BF01143218.

[12] Zweben C. Tensile strength of hybrid composites. J Mater Sci 1977;12:1325–37. doi:10.1007/BF00540846.

[13] Harlow DG, Phoenix SL. The chain-of-bundles probability model for the strength of fibrous materials II: a numerical study of convergence. J Compos Mater 1978;12:314–34.

[14] Jr. LM, Brøndsted P. Micromechanical modeling of damage and fracture of unidirectional fiber reinforced composites: A review. Comput Mater Sci 2009;44:1351–9. doi:http://dx.doi.org/10.1016/j.commatsci.2008.09.004.

[15] Tavares RP, Melro AR, Bessa MA, Turon A, Liu WK, Camanho PP. Mechanics of hybrid polymer composites : analytical and computational study. Comput Mech 2016;57:405–21. doi:10.1007/s00466-015-1252-0.

[16] Okabe T, Sekine H, Ishii K, Nishikawa M, Takeda N. Numerical method for failure simulation of unidirectional fiber-reinforced composites with spring element model. Compos Sci Technol 2005;65:921–33. doi:http://dx.doi.org/10.1016/j.compscitech.2004.10.030.

[17] Okabe T, Ishii K, Nishikawa M, Takeda N. Prediction of Tensile Strength of Unidirectional CFRP Composites. Adv Compos Mater 2010;19:229–41. doi:10.1163/092430409X12605406698273.
[18] Swolfs Y, Gorbatikh L, Verpoest I. Fibre hybridisation in polymer composites: A review. Compos Part A Appl Sci Manuf 2014;67:181–200. doi:http://dx.doi.org/10.1016/j.compositesa.2014.08.027.
[19] Fukuda H. An advanced theory of the strength of hybrid composites. J Mater Sci 1984;19:974–82. doi:10.1007/BF00540468.
[20] Jr. LM, Dai G. Hybrid carbon/glass fiber composites: Micromechanical analysis of structure--damage resistance relationships. Comput Mater Sci 2014;81:630–40. doi:http://dx.doi.org/10.1016/j.commatsci.2013.08.024.
[21] Swolfs Y, McMeeking RM, Verpoest I, Gorbatikh L. The effect of fibre dispersion on initial failure strain and cluster development in unidirectional carbon/glass hybrid composites. Compos Part A Appl Sci Manuf 2015;69:279–87. doi:http://dx.doi.org/10.1016/j.compositesa.2014.12.001.
[22] Melro AR, Camanho PP, Pinho ST. Generation of random distribution of fibres in long-fibre reinforced composites. Compos Sci Technol 2008;68:2092–102. doi:http://dx.doi.org/10.1016/j.compscitech.2008.03.013.
[23] Nishikawa M, Okabe T, Takeda N. Determination of interface properties from experiments on the fragmentation process in single-fiber composites. Mater Sci Eng A 2008;480:549–57. doi:10.1016/j.msea.2007.07.067.
[24] Curtin WA. Tensile Strength of Fiber-Reinforced Composites: III. Beyond the Traditional Weibull Model for Fiber Strengths. J Compos Mater 2000;34:1301–32.
[25] Watson AS, Smith RL. An examination of statistical theories for fibrous materials in the light of experimental data. J Mater Sci 1985;20:3260–70. doi:10.1007/BF00545193.
[26] Padgett WJ, Durham SD, Mason AM. Weibull Analysis of the Strength of Carbon Fibers Using Linear and Power Law Models for the Length Effect. J Compos Mater 1995;29:1873–84.